

BRAZING FREE RF PULSE COMPRESSOR FOR HIGH GRADIENT ACCELERATORS

L. Kankadze*¹, D. Alesini, F. Cardelli, M. Diomedede, G. Di Raddo
 INFN - Laboratori Nazionali di Frascati, Frascati, Italy
¹also at Kutaisi International University, Kutaisi, Georgia

Abstract

EURPRAXIA@SPARC_LAB, is a proposal to upgrade the SPARC_LAB test facility (at LNF, Frascati) to a soft X-ray user facility based on plasma acceleration and high-gradient X-band (11.9942 GHz) accelerating modules. Each module is made up of a group of 4 TW sections assembled on a single girder and fed by one klystron by means of one rf pulse compressor system and a low attenuation circular waveguide network that transports the rf power to the input hybrids of the sections.

The pulse compressor is based on a single Barrel Open Cavity (BOC). The BOC use a “whispering gallery” mode which has an intrinsically high quality factor and operates in a resonant rotating wave regime. Compared to the conventional SLED scheme it requires a single cavity instead of two cavities and a 3-dB hybrid. A new brazeless mechanical design has been proposed and is described in the present paper together with the electro-magnetic and thermo-mechanical simulations.

INTRODUCTION

The BOC pulse compressors operate with $TM_{m,1,1}$ -like modes, where m is the azimuthal index. The sketch of a typical BOC cavity with main dimensions is given in Fig. 1 a). The quality factors Q_0 of these modes are equal to a/σ where a is the large radius in the middle plane and σ is the skin depth. The Q_0 value is defined by the azimuthal index of the mode and therefore by the diameter of the cavity [1]. For a first prototype we have chosen to operate with a $TM_{16,1,1}$ mode and a coupling coefficient equal to 7.8 These parameters have been chosen according to the procedure illustrated in [2] and in order to maximize the effective shunt impedance of the accelerating structures.

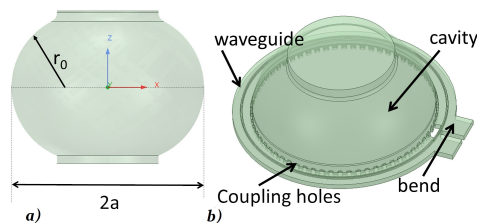


Figure 1: a) A sketch of BOC profile b) Geometry simulated in ANSYS-HFSS.

* levan.kankadze@kiu.edu.ge

BRAZELESS ASSEMBLY OF STRUCTURES

Accelerating cavities are usually made of many single cells welded together. The most common welding techniques is the brazing, in which a metal alloy is melted and distributed by capillarity between the two surfaces to be joined. This high-temperature processes require high-level skills, expensive vacuum furnaces and have a non-negligible probability of failure. A novel fabrication procedure for accelerating structures has been recently developed at LNF-INFN [3,4]. It involves special gaskets that guarantee (simultaneously) the vacuum seal and perfect rf contact when the structure is clamped. This procedure allows to avoid brazing process with a contemporary reduction of cost and delivery time. Moreover non-annealed copper has been demonstrated to sustain higher peak electric field [5].

This procedure has been applied so far to rf-guns in S-band [3, 6]. The present paper is focused on the design of a BOC cavity that allows to implement for its realization the brazing-free technology.

ELECTROMAGNETIC DESIGN

The electromagnetic (e.m.) simulations have been done using ANSYS-HFSS [7]. The simulated geometry is given in Fig. 1. The following subsections summarize the design process.

Eigenmode Simulations

By eigenmode simulations of one slice of the whole cavity with proper boundary conditions as given in Fig. 2, we have tuned the resonant frequency (11.9942 GHz) and evaluated the quality factor 143 000 These results have been in perfect agreement with the theoretical expectations.

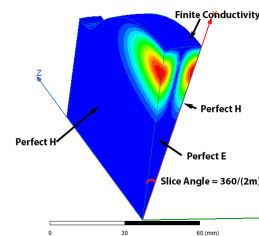


Figure 2: Slice with angle value and boundary conditions.

Input Waveguide and Bend

The two cavity modes in the BOC can be excited by means of multi-hole coupling slots through the common wall be-

tween the cavity and a waveguide, which surrounds the entire cavity at its median plane, as sketched in Fig. 3. The wavelength in the waveguide is designed to be equal to the distance between the BOC mode lobes [1] while the number of coupling holes to excite one mode polarity is typically chosen exactly equal to $2m$ in order to maximize the coupling effectiveness itself. The input bend allows to properly connect the waveguide with the waveguide network.

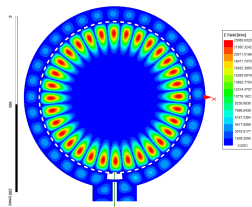


Figure 3: Electric field in the cavity and waveguide.

To allow a realization of the structure with the gaskets-clamping technique, a gap has been introduced in the center of the waveguide and bend as sketched in Fig. 4 a). This gap, if properly designed, doesn't affect the TE_{01} field distribution in the waveguide, but gives the possibility to clamp the structure avoiding any brazing. Also, the increase of the electric field magnitude due to the presence of the gap itself can be taken under control by a proper design of the rounded corners.

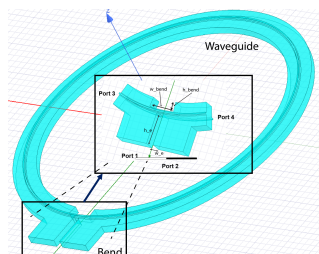


Figure 4: Waveguide a) with bend b).

The gap's width w_{gap} has been reduced up to 1 mm in order to reduce the electric field penetration in the gap itself and, at the same time, the electric field increase due to the gap itself. For this last reason also rounded corners of radius r equal to 0.5 mm have been introduced. This gives an increase of the surface electric field on the corner with respect to the unperturbed waveguide of the order of 40% if the gap is inserted exactly in the center of the waveguide. In the first version of the design we adopted this central position but it is possible to reduce this effect by an off center position of the gap itself Fig. 5.

For the same reasons of fabrication with clamping, an aperture between the two waveguides in the bend has been inserted Fig. 4 b). We verified by simulation that the crosstalk between the two waveguides due to this aperture is completely negligible. The final bend design showed a reflection coefficient < -35 dB.

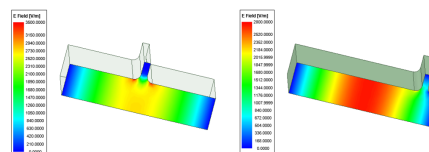


Figure 5: Electric field inside the waveguide for different gap positions.

Coupling Factor

As pointed out, coupling between the waveguide and cavity is realized by means of coupling slots. Coupling strength depends on slot dimensions and the common wall thickness between the waveguide and the cavity. In our case wall thickness was set equal to 2 mm. To reach the desired coupling factor HFSS simulations have been done and the slot's width was gradually increased until desired result has been reached. The coupling factor as a function of the slot width is given in Fig. 6 and the desired coupling of 7.8 has been reached with a width of 3.8 mm. The final magnitude of the electric field on the middle plane is reported in Fig. 3.

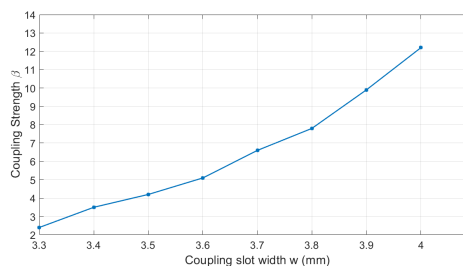


Figure 6: Coupling factor versus coupling width.

THERMO-MECHANICAL SIMULATIONS

To properly design the cooling pipes and keep the BOC detuning under powering under control, thermo-mechanical simulations in ANSYS-WORKBENCH have been carried out. These simulations allow to combine the electromagnetic simulation with the thermo-mechanical analysis. The power dissipated in the BOC is in our case equal to 1.6×10^3 W. The cooling water temperature was set to 22 °C. Maximum temperature increase occurred on the coupling slots, where field is maximum, as expected, with an increase up to 25.5 °C as reported in Fig. 7. We verified with the combined electromagnetic simulations that the change in the resonant frequency and BOC parameters due to this heating is completely negligible.

BOC Final Parameters

The scattering parameters are given on Figs. 8 and 9, S_{11} is below < -25 dB while the coupling coefficient is equal 7.8. The final parameters of the pulse compressor are summarized in the Table 1.

Content from this work may be used under the terms of the CC BY 3.0 licence (© 2021). Any distribution of this work must maintain attribution to the author(s), title of the work, publisher, and DOI

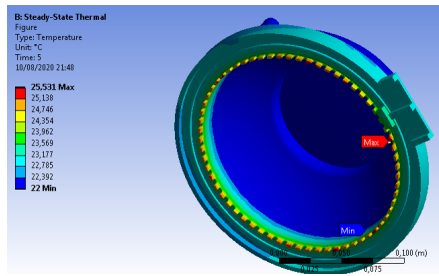


Figure 7: Temperature distribution on the BOC pulse compressor at full power.

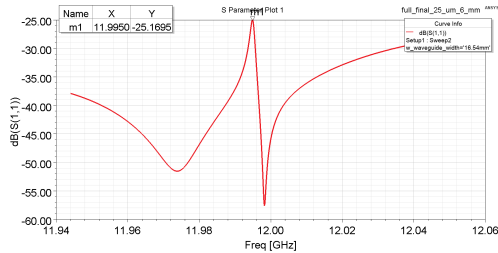


Figure 8: Reflection coefficient at the waveguide input port as a function of frequency for the final simulated structure.

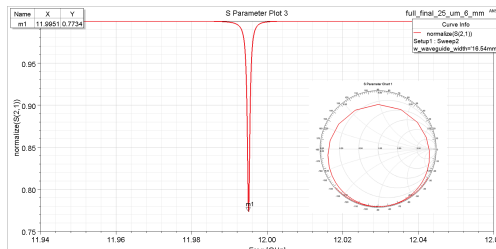


Figure 9: Magnitude of the S_{21} as a function of frequency and Smith chart of the transmission coefficient S_{21} .

Table 1: Main Parameters of BOC

Pulse compressor	Design parameter
Type	Barrel Open Cavity
Frequency	11.9951 GHz
Resonant mode	$TM_{16,1,1}$
Diameter	171.3 mm
Q	143 000
Coupling factor (β)	7.8
Input power	50 MW
Repetition rate	100 Hz
Average dissipated power	1.6 kW

MECHANICAL DESIGN

The mechanical design of the structure has been performed with the commercial CAD code Autodesk Inventor [8]. The structure consists from two main parts: the body of the cavity with half of the waveguide and waveguide with the bend Fig. 10. These two parts are joined with two aluminum gaskets and fasteners. The aluminum gaskets are not exposed to RF.

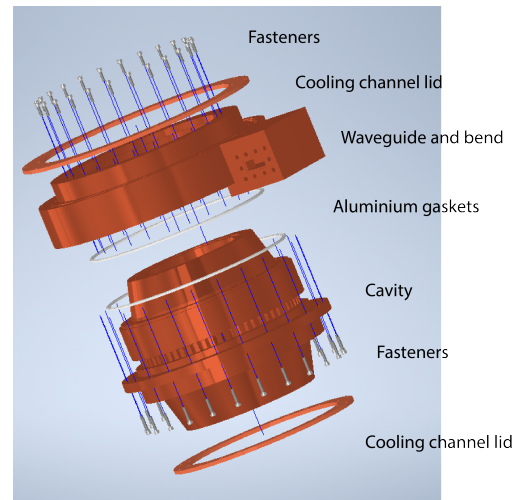


Figure 10: 3D mechanical model.

CONCLUSION

The new BOC design we proposed with the possibility to fabricate a clamped device has several advantages. First of all, the realization does not require expensive processes in vacuum furnaces with a reduction of the realization cost. The use of hard copper instead of annealed one allows to obtain, in principle, even better performances at high power. With this technology it is also possible to open the structure, machine it to reach the desired resonant frequency, and close it again with a reduction of the required precision in the fabrication of the device and overall cost.

REFERENCES

- [1] I. V. Syrachev, "The Progress of X-Band Open" Cavity RF Pulse Compression Systems", in *Proc. 4th European Particle Accelerator Conf. (EPAC'94)*, London, UK, Jun.-Jul. 1994, pp. 375–380.
- [2] M. Diomedè, "High-gradient structures and rf systems for high-brightness electron linacs", thesis, Università degli studi di Roma-La Sapienza, Rome, Italy, Jan. 2020.
- [3] D. Alesini *et al.*, "New technology based on clamping for high gradient radio frequency photogun", *Phys. Rev. ST Accel. Beams*, vol. 18, no. 9, p. 092001, 2015. doi:10.1103/PhysRevSTAB.18.092001
- [4] D. Alesini *et al.*, "Process for manufacturing a vacuum and radio-frequency metal gasket and structure incorporating it", PATENT No. WO2016147118A1, 2016.
- [5] V. A. Dolgashev, "Progress on high-gradient structures", *AIP Conference Proceedings*, vol. 1507, no. 1, Dec. 2012. doi:10.1063/1.4773679
- [6] D. Alesini *et al.*, "Design, realization, and high power test of high gradient, high repetition rate brazing-free S-band photogun", *Phys. Rev. Accel. Beams*, vol. 21, no. 11, p. 112001, 2018. doi:10.1103/PhysRevAccelBeams.21.112001
- [7] ANSYS-HFSS, <https://www.ansys.com/>.
- [8] Autodesk Inventor, <https://www.autodesk.com/>.